

Personal Exposimeter for Radio Frequency Exposure Assessment in the 60-GHz Band

Reza Aminzadeh¹, Arno Thielens¹, Haolin Li¹, Carole Leduc², Maxim Zhadobov², Guy Torfs¹, Johan Bauwelinck¹, Luc Martens¹, and Wout Joseph¹

¹Department of Information Technology, Ghent University / iMinds, Ghent, Belgium

²Institutes of Electronics and Telecommunications of Rennes (IETR), University of Rennes 1, France

*Corresponding author e-mail: Reza.Aminzadeh@intec.UGent.be

SHORT ABSTRACT

For the first time a personal Exposimeter (PE) is presented for radiation assessment in the 60-GHz band. Numerical simulations are used to design the PE and its uncertainty is assessed using on-body calibration measurements at 61 GHz. The PE consisting of three nodes (antennas) with vertical-horizontal-horizontal (VHH) polarization has a 50% prediction interval of 1.3 dB which is 3.1 dB lower than a single node experiment. The proposed PE has a 19.7 dB smaller uncertainty compared to the currently available exposimeters at lower frequencies. A 95 % confidence interval of 6.6 dB is measured on the response of the proposed PE.

INTRODUCTION

The increasing demand for new wireless technologies and rapid progress in 60 GHz wireless communication systems have increased the concerns about potential health effects of mm-waves on human body [1, 2]. In order to ensure that mm-wave systems have no adverse health effects on the users, compliance with international guidelines such as those issued by ICNIRP [2] is necessary. Since the absorption of mm-waves is limited to the human skin [3] the incident power density (IPD) is studied as a dosimetric quantity at mm-waves. The safety limits of IPD are 1 mW/cm² and 5 mW/cm² averaged over 20 cm² of the exposed area for general public and occupational exposure, respectively. Personal exposimeters (PEMs) are used to measure the IPD at lower frequencies [4]. The performance of these devices is affected by the reflection and absorption of the human body, which results in a relatively large measurement uncertainty [5]. Moreover, it was shown that the location of the PEM on the subject's body can cause large measurement uncertainties [6]. Previous dosimetric studies in the 60-GHz band, for example [7], have only investigated the exposure of biological cells at 60 GHz. A prototype of wearable on-body exposimeter (PE) for the millimeter wave band is presented. The PE consists of three receiving antennas and can be used to measure the incident power density in realistic indoor environments, and is calibrated in anechoic conditions using a real human subject.

MATERIALS AND METHODS

This study consists of two parts: numerical simulations and calibration measurements on a real human subject. The goal is to determine the response of the proposed PE in the 60-GHz band as well as its measurement uncertainty.

Numerical modeling

The response of the PE (on body) is studied using the Finite-Difference Time-Domain (FDTD) simulations. The antenna used in this study is a four-patch antenna array that has a power reflection coefficient of lower than -10 dB in the 55-65 GHz range [8]. In order to emulate the human body, a homogeneous single-layer skin model is proposed (200×200×10

mm³). The reason is shallow penetration depth of mm-waves in the skin [1]. The dielectric properties of dry skin [9] are assigned to the proposed numerical model. The antenna is placed at 5.6 mm from the skin model due to the geometry of the connector used in measurements. In order to determine the response of the antenna, simulations are performed for the antenna with and without the skin model. The quantity studied here is the response (R) of the PE which is the ratio of the median on-body received power (P_r^{body}) to the median received power in free space (P_r^{free}):

$$R = 10 \times \log \left(\frac{P_r^{body}}{P_r^{free}} \right) \quad (1)$$

The received power on an antenna can be determined from its aperture [10]:

$$P_r(\varphi, \theta) = AA(\varphi, \theta) \times S_{inc} \quad (2)$$

where $AA(\varphi, \theta)$ and S_{inc} are the on-body aperture of the antenna and incident power density, respectively. Using the method described in [11], first, the on-body antenna aperture is determined from its radiation pattern. Next, the received power on the antenna is determined by combining different single plane waves using sets of multiple plane waves to calculate the received power on the antenna. A realistic far-field exposure scenario in the 60-GHz band (conference room of IEEE 802.11) is considered [12].

Calibration measurements

The calibration measurements are performed using the measurement setup in Figure 1. First, the free-space incident power density is calculated using the Friis formula [10] and is averaged over 20 cm² of the studied area [3]. Second, the patch antenna array is used as a receiver (RX) on a male subject's forearm and the received power on the RX is measured on 5 locations (for five φ angles). Two orthogonal polarizations of the antennas are studied, horizontal (H) and vertical (V). Third, three locations are selected for mounting the RX on the subject's forearm (see Figure 2) and the second step is repeated to obtain the best combination of three antennas (lowest measurement uncertainty). Using equation (2) the effective median on-body antenna aperture is obtained from calibration measurements. Next, AA values are determined for any realistic polarization [12]. These AA values can be used in realistic environments to determine the incident power density from the measured received power.

RESULTS AND DISCUSSION

Using equation (1) the simulated and measured (for single antenna) responses are determined and are equal to 0.72 (-1.4 dB) and 0.8 (-0.96 dB), respectively, which shows a good agreement. The median AA values are 9.2 mm², 7.7 mm² and 2.3×10^{-3} mm² for horizontal orientation of RX on body, simulated horizontal RX on the skin model, and vertical RX on body, respectively. The simulated and measured AA values are in good agreement (difference of 17.7%). The lower simulated AA value indicates higher received power and is due to the exclusion of the connector. Also the difference between H and V orientation of the RX can be interpreted as the asymmetric structure of the RX and strong dependence of reflection and transmission coefficients at mm-waves. Figure 3 shows the 50% (PI_{50}) and 95% (PI_{95}) prediction intervals of the response of the PE consisting of 1, 2 and 3 antennas. The value of PI_{50} improved 3.1 dB for three antennas (4.4 dB) compared to one antenna (1.3 dB). Our proposed exposimeter has an improved PI_{50} of 16.6 dB (1 antenna) and 19.7 dB (3

antennas) compared to the PI_{50} of commercial PEMs (up to 21 dB) at lower frequencies (≤ 6 GHz) [5]. Also the PI_{95} value has an 8.8 dB improvement for 2 and 3 antennas (6.6 dB) compared to a single antenna (15.4 dB). The PI_{95} is 11.9 dB lower than the PI_{95} of a commercial exposimeter in an indoor scenario (18.5 dB at 900 MHz) [13].

ACKNOWLEDGEMENT

This research was funded by the Research Foundation-Flanders (FWO-V) under grant agreement No G027714N.

REFERENCES

- [1] Zhadobov M, Chahat N, Sauleau R, Le Quement C, Le Drean Y. 2011. Millimeter-wave interactions with the human body: state of knowledge and recent advances. *International Journal of Microwave and Wireless Technologies* 3 (2):237-247.
- [2] Wu T, Rappaport T, Collins C. 2015. Safe for generations to come: Considerations of safety for millimeter waves in wireless communications. *Microwave Magazine IEEE*, 16(2): 65-84.
- [3] International Commission on Non-Ionizing Radiation Protection. 1998. Guidelines for limiting exposure to time-varying electric, magnetic, and electromagnetic fields (up to 300 GHz). *Health Physics* 74: 494-522.
- [4] Frei P, Mohler E, Neubauer G, Theis G, Bürgi A, Fröhlich J, Braun-Fahrlander, Bolte J, Egger M, Rösli M. 2009. Temporal and spatial variability of personal exposure to radio frequency electromagnetic fields. *Environmental Research* 109(6): 779-785.
- [5] Bolte JFB, Van der Zande G, Kamer J, 2011. Calibration and uncertainties in personal exposure measurements of radio frequency electromagnetic fields. *Bioelectromagnetics* 32(8): 652-663.
- [6] Gryz K, Zradzinski P, Karpowicz J. 2015. The Role of the Location of Personal Exposimeters on the Human Body in Their Use for Assessing Exposure to the Electromagnetic Field in the Radiofrequency Range 98–2450 MHz and Compliance Analysis: Evaluation by Virtual Measurements. *BioMed Res. Int.* 2015 (272460).
- [7] Zhadobov M, Sauleau R, Augustine R, Le Quement C, Le Drean Y, Thouroude D. 2012. Near-field dosimetry for in vitro exposure of human cells at 60 GHz. *Bioelectromagnetics* 33(1): 55-64.
- [8] Chahat N, Zhadobov M, Le Coq L, Alekseev S, Sauleau R. 2012 Characterization of the interactions between a 60-GHz antenna and the human body in an off-body scenario. *Antennas and Propagation, IEEE Transactions on* 60 (12): 5958–5965.
- [9] Gabriel C, Gabriel S, Corthout E. 1996. The dielectric properties of biological tissues. *Phys Med Biol* 41:2231-2293.
- [10] Balanis CA. 2005. *Antenna Theory: Analysis and Design*. 3rd ed., Wiley, Hoboken, NJ.
- [11] Aminzadeh R, Thielens A, Bamba A, Kone L, Gaillot D, Lienard M, Martens L, Joseph W. 2015. On-body calibration and measurements using personal radio-frequency exposimeters in indoor diffuse and specular environments. *Bioelectromagnetics*, submitted for publication.
- [12] Maltsev A, Erceg V, Perahia E, Hansen Ch, Maslennikov R, Lomayev A, Sevastyanov A, Khoryaev A, Morozov G, Jacob M, Priebe S, Kürner Th, Kato Sh, Sawada H, Sato K, Harada, H. 2010. Channel models for 60 GHz WLAN Systems. Tech. Rep. IEEE 802.11-09/0334r8. Available: <https://mentor.ieee.org/802.11/dcn/09/11-09-0334-08-00ad-channel-models-for-60-ghz-wlan-systems.doc>
- [13] Iskra S, McKenzie R, Cosic I. 2011. Monte Carlo simulations of the electric field close to the body in realistic environments for application in personal radiofrequency dosimetry. *Radiat Prot Dosim* 147(4):517-527.

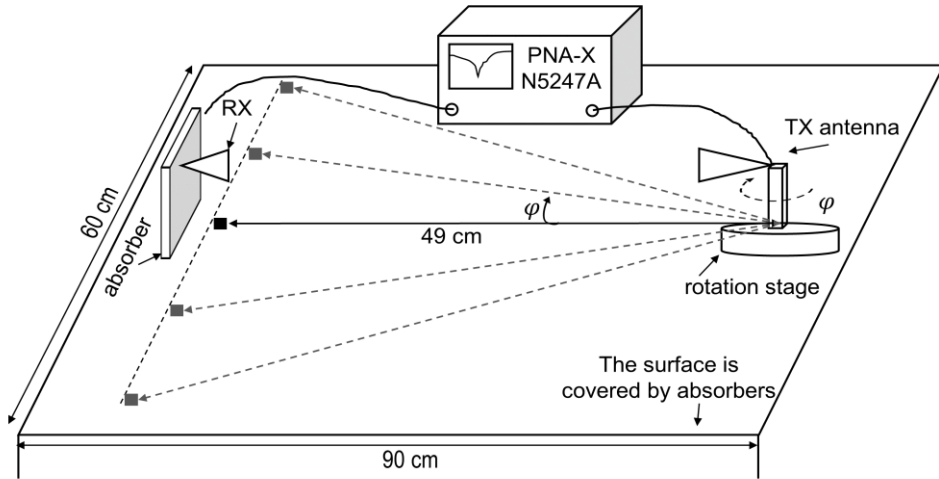


Figure. 1: Measurement setup used for calibration measurements. Solid squares show five locations of RX.

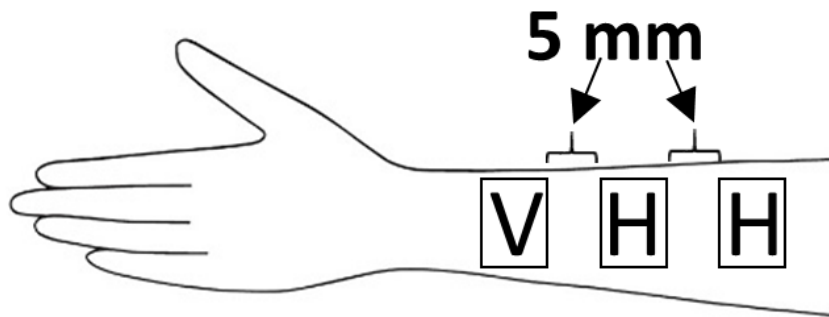


Figure. 2: The optimized orientation of the receiver nodes on the subject's forearm.

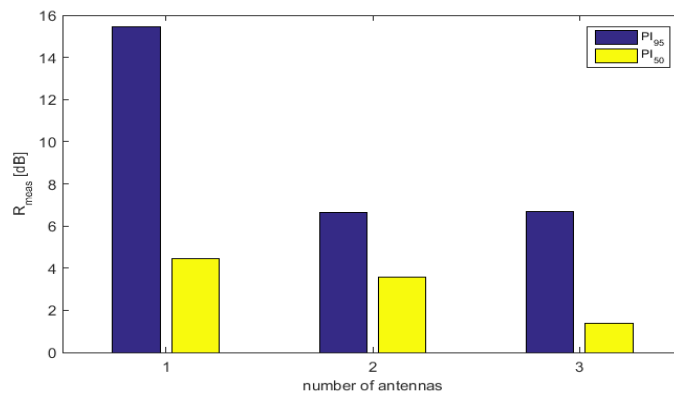


Figure. 3: The 50 % and 95 % prediction intervals of the averaged response for the optimized combination of three antennas.